Corrosion inhibition of 6063 aluminum alloy by *Coriandrum sativum L* seed extract in phosphoric acid medium

Deepa Prabhu and Rao Padmalatha [*]

[1]*Department of Chemistry, Manipal Institute of Technology, Manipal University, Karnataka 576104, India.*

Abstract

Coriandrum sativum L. seed extract (CSE) was used as a green inhibitor for corrosion control of 6063 aluminium alloy in 1 M phosphoric acid using potentiodynamic polarization and electrochemical impedance spectroscopy (EIS) techniques at the temperature range of 30°C to 50°C. Surface morphology of the metal was studied using Scanning electron microscopy (SEM), both in the absence and in the presence of inhibitor. Inhibition efficiency increased with extract concentration and decreased with temperature. Inhibitor acted as mixed type of inhibitor. The adsorption of CSE on alloy surface was fit into Langmuir adsorption isotherm. Kinetic and thermodynamic parameters governing the adsorption process were calculated and discussed in detail. Results obtained by Tafel polarisation method and electrochemical impedance spectroscopy method were in good agreement with one another. SEM studies confirmed the corrosion inhibition of the alloy due to the adsorption of CSE. CSE emerged as a biodegradable, environmentally benign green inhibitor with minimal health and safety concerns. It has the potential to be a cost effective alternative to synthetic corrosion inhibitors. It can be treated as effective tool to preserve environmental burden of harmful synthetic organic inhibitor.

Key words: Green inhibitor, Aluminium alloy, phosphoric acid, *Coriandrum sativum L.*, Electrochemical technique, SEM.

1. Introduction

Corrosion studies of aluminium and aluminium alloys have received considerable attention by researchers because of their technological importance and industrial applications. They find applications in automobiles, aviation, household appliances, containers and electronic devices [1, 2]. Although pure aluminium is too soft to be used as a heavy duty material for large structures, high strength aluminium alloys can be produced by addition of appropriate alloying elements such as silicon [3]. The applications of aluminium and its alloys are often possible because of the natural tendency of aluminium to form a passivation oxide layer. However, in aggressive media, the passivation layer can be destroyed and corrosion attack can take place. The protection of aluminium and its oxide films against the corrosive action of chloride ions have been extensively studied [4-6].The breakdown of the passivation oxide films on aluminium and its alloys by these ions are frequently responsible for the failure of the articles.

Phosphoric acid is a major industrial chemical. Electronic industry uses phosphoric acid in the preparation of semiconductors and printed circuit boards. It is also used to remove mineral deposits from the process equipment and boilers. It is widely used for acid pickling and electro polishing of aluminium [7] but it shows strong corrosiveness on aluminium and its alloys.Therefore it is necessary to seek inhibitors for the corrosion of aluminium in phosphoric acid.

The protection of metals against corrosion by phosphoric acid has been the subject of much study since it has been used in many industrial processes [8, 9]. Among the several methods of corrosion control and prevention, the use of corrosion inhibitors is very popular. B. Sanyal [10] in his review has given a detailed account of organic corrosion inhibitors including the classification and mechanism of action. Corrosion inhibition potential is mainly attributed to the donation of lone pair of electron from heteroatom to metal atoms. A number of heterocylic compounds have been reported as corrosion inhibitors and the screening of synthetic heterocylic compounds still being continued [11-14].

But unfortunately most of these compounds are not only expensive but also toxic to living beings. It is needless to point out the importance of cheap, safe inhibitors for corrosion. Plant extracts have become important as an environmentally acceptable, readily available and renewable source for wide range of inhibitors. Many reviews

are available in the literature, describing the inhibition effect of numerous plant products on the corrosion of various metals in acidic and alkaline media [15-17].

As a contribution to the current interest of environment friendly corrosion inhibitor, our present investigation aims to introduce *Coriandrum sativum* L as a novel inhibitor for corrosion control of 6063 aluminium alloy in 1M phosphoric acid.

Coriandrum sativum L. known as Coriander is an annual herb in the family of Apiaceae. Dried seeds are most traditionally used in cooking. It is a rich source of antioxidant and has lots of medicinal applications. *Coriandrum sativum* L. contains several biodegradable ecologically acceptable organic compounds [18]. References are available for using *Coriandrum sativum* L. as inhibitor for the corrosion control of steel in acid medium [19]. No reported literature is available for using the same for the corrosion control of 6063 aluminium alloy in phosphoric acid medium by electrochemical techniques.

2. Materials and methods

2.1 Material

The commercially available sample of 6063 aluminium alloy was used for the study. The composition of the specimen is given in Table1.

Table 1: Composition of the 6063 aluminium alloy specimen

Element	Composition
Si	0.41%
Fe	0.11%
Cu	0.05%
Mg	0.49%
Al	Balance

2.2 Medium

Stock solution of 1.0M phosphoric acid was prepared by diluting AR grade phosphoric acid (85%) with double distilled water. It was standardized by potetniometric method.

2.3 Preparation and Characterization of Coriandrum sativum L. extract (CSE)

Dried seeds of *Coriandrum sativum* L. were finely powdered and aqueous extract was prepared by taking 10g of finely powdered seeds in 100ml of distilled water and refluxed for 3hours [20]. It was filtered and the filtrate was evaporated to dryness. Dried powder was preserved in a desiccator. It was used to prepare the aqueous inhibitor solution of required strength. The concentration range of CSE used was 100-500 ppm.

FTIR spectra of the dried sample were recorded using spectrophotometer (Shimadz Model) in the frequency range of 4000 to 400 cm^{-1} using KBr pellets.

2.4 Electrochemical measurements

Cylindrical test coupon was sealed with Acrylic resin material in such a way that the area exposed to the medium was 1.0 cm^2. The coupon was polished with 180, 280, 400, 600, 800, 1000, 1500, and 2000 grade emery papers. Further polishing was done with a disc polisher using levigated alumina to obtain mirror surface. It was dried and stored in a desiccator to avoid the contact with moisture before used for corrosion studies.

Electrochemical measurements were carried out by using an electrochemical work station, (CH600D-series, U.S. Model with CH instrument beta software). The electrochemical cell used was a conventional three electrode compartment Pyrex glass cell with a platinum counter electrode and a saturated calomel electrode (SCE) as reference. The working electrode was made up of 6063 aluminium alloy. All the values of potential were with reference to the SCE. The polarization studies were done immediately after the EIS studies on the same electrode without further surface treatment. Finely polished specimen was exposed to the corrosion medium of 1.0M phosphoric acid in the absence and in the presence of the inhibitor at different temperatures (30° to 50°C) and allowed to establish a steady-state open circuit potential (OCP). The potentiodynamic current–potential curves were recorded by polarizing the specimen to −250 mV cathodically and +250 mV anodically with respect to the OCP at a scan rate of 1 mV s^{-1}.

Inhibitor efficiency was calculated using the relation:

$$\eta(\%) = \frac{i_{corr} - i_{corr(inh)}}{i_{corr}} \times 100$$

(1)

Where i_{corr} and $i_{corr\,(inh)}$ are the corrosion current densities obtained in uninhibited and inhibited solutions, respectively. The corrosion rate was calculated using equation (2):

$$\upsilon_{corr}\left(\text{mm y}^{-1}\right) = \frac{3270 \text{ x } M \text{ x } i_{corr}}{\rho \text{ x } Z}$$

$$(2)$$

Where 3270 is a constant that defines the unit of corrosion rate, i_{corr} is the corrosion current density in A cm^{-2}, ρ is the density of the corroding material (g cm^{-3}), M is the atomic mass of the metal and Z is the number of electrons transferred per atom.

The impedance measurements were carried out in the frequency range from 100 kHz to 0.01 Hz, at the rest potential, by applying 10 mV sine wave AC voltage. The impedance data were analyzed using Nyquist plots. The polarization resistance, R_p, was extracted from the diameter of the semicircle in Nyquist plot.

Percentage efficiency of the inhibitor was calculated using relation:

$$\eta(\%) = \left(\frac{R_{p(inh)} - R_p}{R_{p(inh)}}\right)$$

$$(3)$$

$R_{p\ (inh)}$ and R_p are the polarization resistances in the presence and absence of inhibitor.

In both the methods minimum of three trails were done and average of these trails was reported.

3. Results and discussion

3.1 Fourier transform infrared (FTIR) spectroscopy of CSE

Fig.1 shows the FTIR spectrum of CSE. –OH stretching frequency appears at 3396.41cm^{-1}. The aromatic stretching frequency appears at 2925.81cm^{-1}. The –C–H stretching frequency at 2447.50 cm^{-1}.–C=O– stretching frequency is at 1612.38 cm^{-1}. –CH$_2$ bending frequency 1413.72 cm^{-1}. –C–H bending frequency at 1261.36 cm^{-1}. –C=C– bending frequency at 1051.13 72 cm^{-1}.
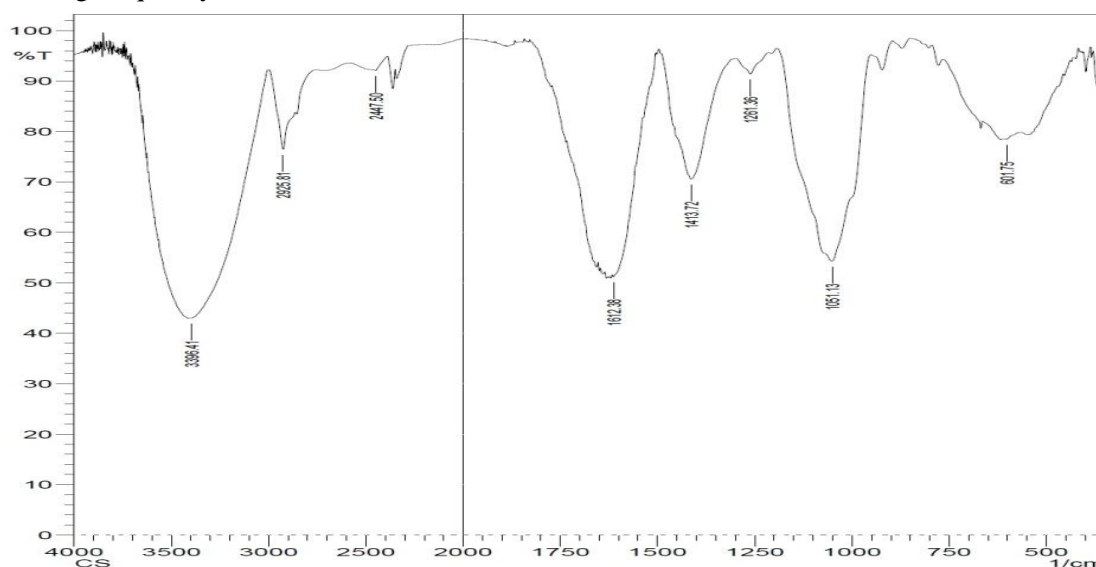

Figure 1: FTIR spectra of solid residue of CSE

3.2 Potentiodynamic polarization curves

Fig. 2 shows the Tafel polarization curves for 6063 aluminium alloy in 1M phosphoric acid solution at different concentrations of inhibitor at 30°C. Similar results were obtained at other temperature as well.

The potentiodynamic parameters such as corrosion potential (E_{corr}), cathodic and anodic Tafel slopes (b_c and b_a), corrosion current density (i_{corr}) were obtained from Tafel plots and the percentage inhibition efficiency η (%), was calculated using equation (1). The results are tabulated in Table 2.

From Fig. 2 and Table 2, it can be observed that the addition of CSE at all the studied concentration resulted in the significant decrease in the corrosion current density (i_{corr}). The decrease in the corrosion density was followed by substantial decrease in the corrosion rate. It is also evident that percentage efficiency of the inhibitor increased with increase in the concentration. Percentage efficiency of the inhibitor also decreased with increase in temperature. There was no remarkable shift in the corrosion potential (E_{corr}) value with respect to the blank. The changes observed in the polarization curves after the addition of the inhibitor are usually used as the criteria to classify inhibitors as cathodic, anodic or mixed [21, 22]. Both anodic and cathodic polarizations are influenced simultaneously, almost to the same extent, which indicate the influence of CSE on both the anodic

and the cathodic reactions; hydrogen evolution and metal dissolution [23]. According to the reported literature [24] if the displacement in corrosion potential is more than ±85 mV with respect to the corrosion potential of the blank, the inhibitor can be considered a distinctive cathodic or anodic type. However, the maximum displacement in this study is less than ±85 mV; and therefore CSE can be considered a mixed-type inhibitor.

Table 2: Results of tafel polarization studies on 6063 aluminium alloy in 1M phosphoric acid containing different concentrations of *Coriandrum sativum* L.

T (°C)	C (ppm)	E_{corr} (V vsSCE)	i_{corr} (x 10^{-5} A cm^{-2})	ba (V dec^{-1})	-bc (V dec^{-1})	CR (mm y^{-1})	IE (%)
30	Blank	-0.76	38.60	3.34	6.72	4.20	---
	100	-0.72	11.39	3.34	6.27	1.24	70.48
	200	-0.72	11.10	3.36	6.18	1.20	71.24
	300	-0.72	10.99	3.37	6.29	1.19	71.52
	400	-0.71	10.88	3.38	6.27	1.18	71.80
	500	-0.71	10.38	3.31	6.44	1.13	73.10
35	Blank	-0.77	50.50	3.43	6.58	5.50	----
	100	-0.74	19.30	3.57	6.02	2.10	61.77
	200	-0.73	18.80	3.45	6.12	2.04	62.76
	300	-0.72	17.20	3.57	6.05	1.87	65.93
	400	-0.72	15.58	3.60	6.01	1.69	69.14
	500	-0.71	15.51	3.55	6.10	1.69	69.27
40	Blank	-0.78	69.20	3.50	6.43	7.54	----
	100	-0.73	31.68	3.68	5.95	3.45	54.21
	200	-0.73	28.47	3.74	5.86	3.10	58.85
	300	-0.72	26.47	3.77	5.88	2.88	61.74
	400	-0.72	26.20	3.78	5.83	2.85	62.12
	500	-0.72	26.18	3.80	5.92	2.85	62.16
45	Blank	-0.80	96.00	3.69	5.97	10.46	----
	100	-0.73	48.96	3.99	5.57	5.33	48.99
	200	-0.73	46.96	3.92	5.68	5.11	51.08
	300	-0.73	44.87	3.95	5.75	4.89	53.26
	400	-0.73	43.55	3.97	5.81	4.74	54.63
	500	-0.73	37.584	3.99	5.74	4.09	60.85
50	Blank	-0.80	135.40	3.79	5.60	14.75	----
	100	-0.75	70.51	4.08	5.52	7.68	47.92
	200	-0.74	70.23	4.11	5.48	7.65	48.13
	300	-0.74	68.20	4.02	5.57	7.43	49.63
	400	-0.74	67.10	3.97	5.51	7.31	50.44
	500	-0.73	65.95	4.00	5.45	7.18	51.29
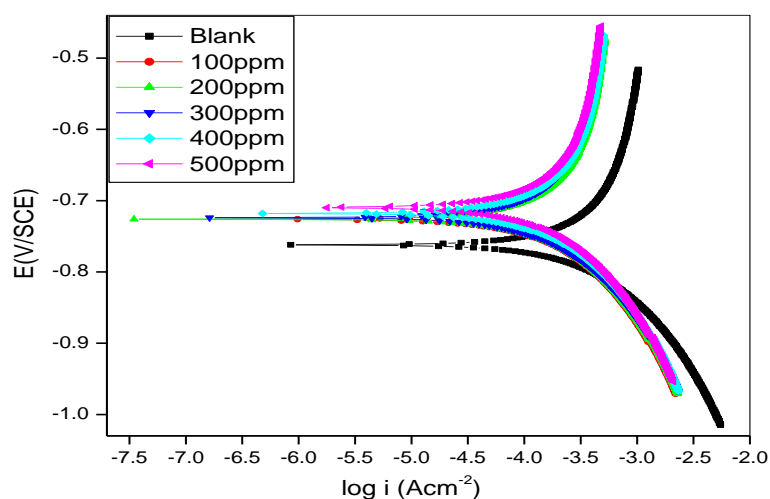
Figure 2: Tafel polarization curves for 6063 Al in 1M H$_3$PO$_4$ solution at different concentrations of inhibitor at 30°C

3.3 Electrochemical impedance spectroscopy (EIS)

The effect of inhibitor concentration on the impedance behaviour of the aluminium in 1M phosphoric acid concentration was studied. Nyquist plot for 6063 aluminium alloy in the absence and in the presence of various concentrations of the inhibitor is given in the Fig. 3. Impedance plots are semicircles both in the absence and in the presence of the inhibitor. The diameter of the capacitive loop increased with increase in the concentration of the inhibitor. This indicates that the impedance of the inhibited substrate increases with the inhibitor concentration. The impedance plots have large capacitive loop at higher frequencies (HF), small inductive loop at intermediate frequencies (IF), followed by a second capacitive loop at low frequency (LF) value for uninhibited surface whereas for inhibited plot consists of the impedance spectra consists of a large capacitive loop at high frequencies (HF) and an inductive loop at low frequencies (LF). The uninhibited plot consists of another capacity loop at lower frequency, whereas after inhibition it is absent due to the adsorption of inhibitor molecule changes the mechanism at the interface. The capacitive loop at HF is related to the charge transfer of the corrosion process and the double layer behaviour [25].
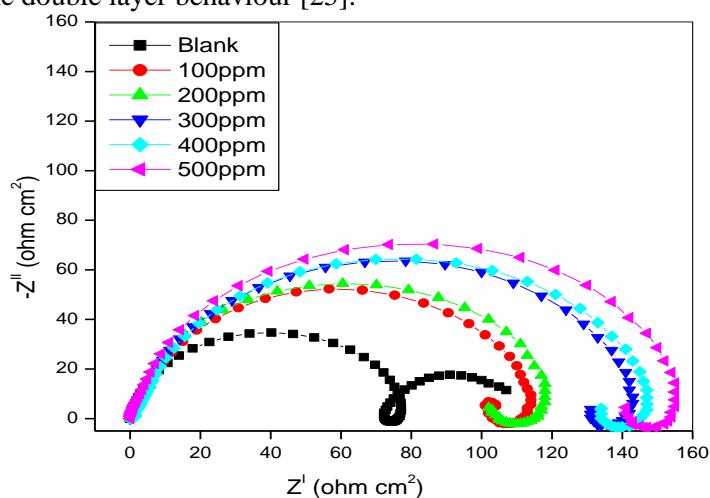
Figure 3: Nyquist plots and equivalent circuit for the corrosion of 6063 aluminium alloy in 1M phosphoric acid containing different concentrations of inhibitor (CSE) at 30°C

The high frequency capacitive loop could be assigned to the charge transfer of the corrosion process and to the formation of oxide layer [23]. The oxide film is considered to be a parallel circuit of a resistor due to the ionic conduction in the oxide film and a capacitor due to its dielectric properties. The capacitive loop is corresponding to the interfacial reactions, particularly the reaction of aluminium oxidation at the metal/oxide/electrolyte interface [26]. The process includes the formation of Al^+ ions at the metal/oxide interface, and their migration through the oxide/solution interface where they are oxidized to Al^{3+}. At the oxide/solution interface, OH^- or O^{2-} ions are also formed. The fact that all the three processes are represented by only one loop could be attributed either to the overlapping of the loops of processes, or to the assumption that one process only dominates, excluding the other processes. The other explanation offered to the high frequency capacitive loop is the oxide film itself. The origin of the inductive loop has often been attributed to surface or bulk relaxation of species in the oxide layer [26]. The LF inductive loop may be related to the relaxation process obtained by adsorption and incorporation of phosphate ions, oxide ions, and charged intermediates on and into the oxide film. The second capacitive loop observed at LF values could be assigned to the metal dissolution.

An equivalent circuit of nine elements depicted in Figure 4a was used to simulate the measured impedance data of the 6063 aluminium alloy. It is shown in Figure 4b. In this equivalent circuit R_s is the solution resistance and R_{ct} is the charge transfer resistance. R_L and L represent the inductive elements. This also consists of constant phase element; CPE (Q) in parallel to the series capacitors C_1, C_2 and series resistors R_1, R_2, R_L and R_{ct}. R_L is parallel with the inductor L. The polarization resistance R_p and double layer capacitance C_{dl} can be calculated from equations (4) and (5):

$$R_p = R_L + R_{ct} + R_1 + R_2 \tag{4}$$

$$C_{dl} = C_1 + C_2 \tag{5}$$

An equivalent circuit of five elements depicted in Fig. 5a was used to simulate the measured impedance data, as shown in Figure 5b for uninhibited metal surface. In this equivalent circuit R_s is the solution resistance and R_{ct} is the charge transfer resistance. R_L and L represent the inductive elements. This also consists of constant phase element; CPE (Q) in parallel to the parallel resistors R_{ct} and R_L, and they are is in series with the inductor L. The polarization resistance R_p can be calculated from: [4] [27].
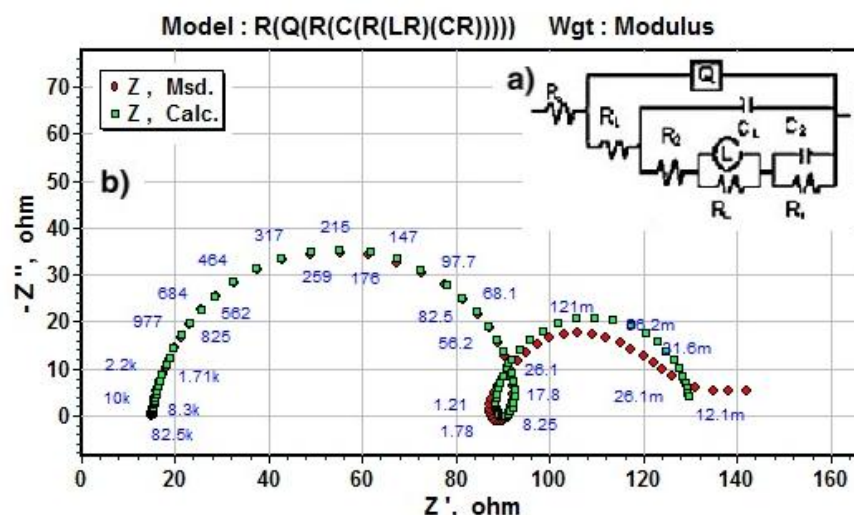
Figure 4: Equivalent circuit used to fit the experimental EIS data for the corrosion of 6063 aluminium alloy specimen in phosphoric acid at 30°C.
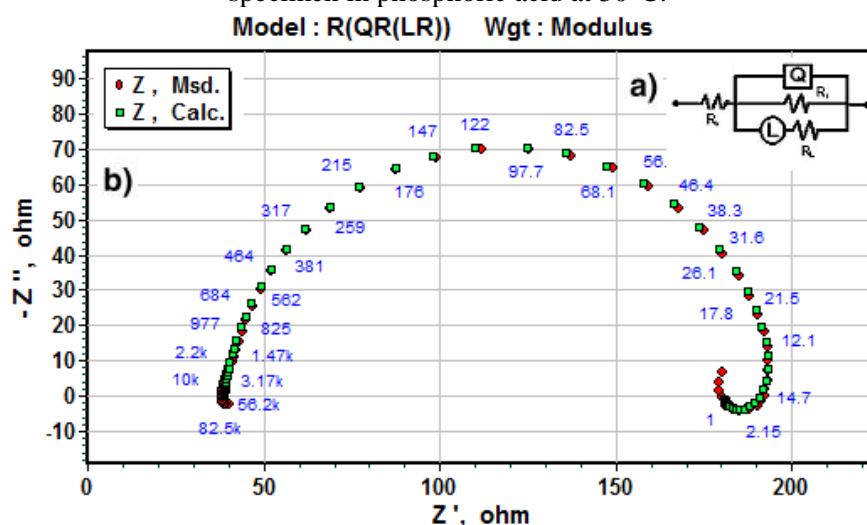
Figure 5: Equivalent circuit used to fit the experimental EIS data for the corrosion of 6063 aluminium alloy specimen in presence of CS at 30°C.

The polarization resistance R_p can be calculated from (6)

$$R_p = \frac{R_L \times R_{ct}}{R_L + R_{ct}}$$

(6)

The circuit fitment was done by ZSimpWin software version 3.21. The results obtained from this are tabulated in Table 3.

The CPE is composed of a component Q_{dl} and a coefficient a. The parameter a quantifies different physical phenomena like surface in-homogeneousness resulting from surface roughness etc., [28]

$$C_{dl} = Q_{dl} \times \left(2\pi f_{max} \right)^{a-1}$$

(7)

The results of Table 3 indicated that, the R_p values increased with the increase in the concentrations of the

inhibitor. As the R_p value increased, there was decrease in the C_{dl} values. Thus effective corrosion resistance was observed to be associated with high R_p and low C_{dl} values [29].

The results of Tafel polarization method and electrochemical impedance method are in good agreement with one another. This proves that corrosion rate depends upon the nature of the inhibitor used and not on the technique employed for measuring the same [30].

Table 3: Electrochemical impedance values of 6063 aluminium alloy in 1M phosphoric acid containing different concentrations of inhibitor at different temperatures

| T (℃)	Conc. (ppm)	R_p (Ω cm^2)	CPE (μ F cm^{-2})	I.E (%)
30	0	101.70	69	
	100	368.38	58	72.39
	200	378.38	45	73.12
	300	382.20	39	73.33
	400	386.09	35	73.63
	500	405.24	32	74.90
35	0	75.90	78	
	100	214.69	65	64.64
	200	220.66	50	65.60
	300	242.12	46	68.65
	400	268.35	41	71.71
	500	269.53	36	71.83
40	0	54.00	90	
	100	129.76	78	58.38
	200	145.52	66	62.89
	300	157.27	58	65.66
	400	158.95	51	66.02
	500	159.13	47	66.15
45	0	36.80	117	
	100	81.74	108	54.98
	200	85.66	89	57.04
	300	90.12	71	59.16
	400	93.15	63	60.49
	500	109.54	58	66.40
50	0	24.20	129	
	100	55.66	115	56.52
	200	55.93	103	56.73
	300	57.89	91	58.20
	400	59.00	82	58.98
	500	60.21	75	59.80

3.4 Effect of temperature

The study on the effect of temperature on the corrosion rate and inhibition efficiency facilitates the calculation of kinetic and thermodynamic parameters for the inhibition and the adsorption processes. These parameters are useful in interpreting the type of adsorption by the inhibitor. The results reported in Table 2 and Table 3 showed that inhibition efficiency of CSE decreased with increase in temperature.

The value of activation energy (E_a) was calculated [31, 32] using the Arrhenius law equation (8):

$$\ln(\upsilon_{corr}) = B - \frac{E_a}{RT} \qquad (8)$$

Where B is a constant which depends on the metal type, R is the universal gas constant, and *T* is the absolute temperature. The plot of ln (υ_{corr}) Vs reciprocal of absolute temperature (1/*T*) gave a straight line with slope = $-E_a$/R, from which the activation energy values for the corrosion process was calculated. The Arrhenius plot for the corrosion of 6063 aluminium alloy in 1M phosphoric acid in the absence and in the presence of different concentrations of inhibitor is shown in Fig. 6.

Deepa and Padmalatha
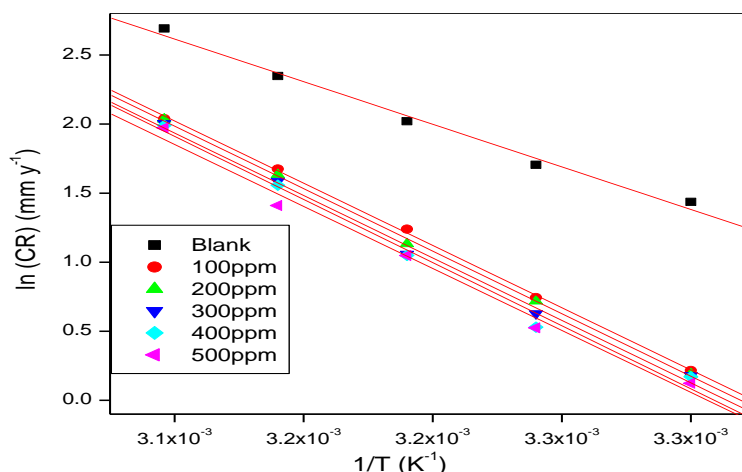
Figure 6: Arrhenius plots for the corrosion of 6063 Al in 1M H_3PO_4 at different concentrations of inhibitor

The Thermodynamic parameters like enthalpy of activation (ΔH_a) and entropy of activation (ΔS_a) were calculated using the transition state equation (9) [33]:

$$\upsilon_{corr} = \frac{RT}{Nh} \exp\left(\frac{\Delta S_a}{R}\right) \exp\left(\frac{\Delta H_a}{RT}\right)$$

(9)

Where h is Plank's constant and N is Avagadro's number. A plot of ln (υ_{corr}/T) vs 1/T gave a straight line with slope $= -\Delta H_a$/T and intercept $= \ln(R/Nh) + \Delta S_a$/R.

The plots of ln (υ_{corr}/T) vs 1/T for the corrosion of 6063 aluminium alloy in the presence of different concentrations of inhibitor are shown in Fig.7. The calculated values of activation parameters are tabulated in Table 4.
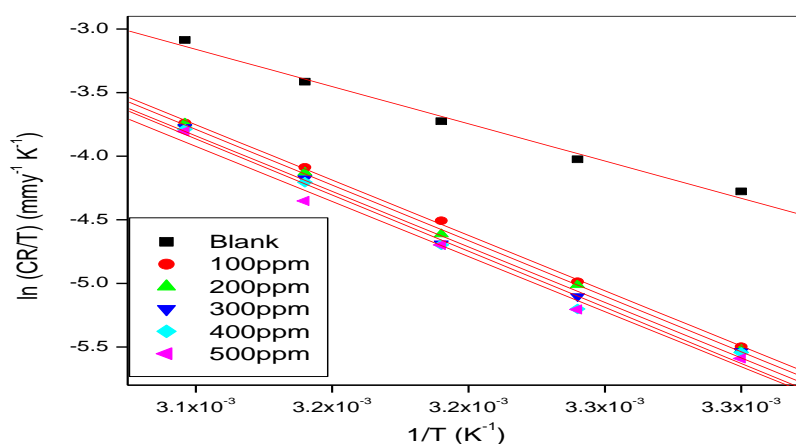
Figure 7: Plots of ln(υ_{corr}/T) vs 1/T for the corrosion of 6063 Al in 1M H_3PO_4 at different concentrations of inhibitor

Table 4: Activation parameters for the corrosion of 6063 Al in 1M H_3PO_4 at different concentrations of inhibitor

Conc. (ppm)	E_a (kJ mol^{-1})	ΔH_a (kJ mol^{-1})	ΔS_a (J mol^{-1} K^{-1})
0.0	50.24	47.69	-72.90
100	74.62	72.01	-69.48
200	74.94	72.34	-45.14
300	75.19	72.58	-44.87
400	75.28	72.67	-37.92
500	75.99	73.38	-21.94

The addition of inhibitor increased the energy of activation value (E_a). This change may be attributed to the change in the mechanism of the corrosion process through physical adsorption in the presence of inhibitor molecules [34]. The energy of activation (E_a) values in the presence of the CSE increased drastically with the

adsorption of components of CSE on the surface of the metal [34, 35]. Large negative values of entropies show that the activated complex in the rate determining step is an association rather than dissociation step meaning that a decrease in disordering takes place on going from reactants to the activated complex [36, 37].

3.5 Adsorption behaviour
In order to understand the mechanism of corrosion inhibition, the adsorption behaviour of the adsorbate on the aluminium surface must be known. The information on the interaction between the inhibitor molecules and the metal surface can be provided by adsorption isotherm. The degree of surface coverage (θ) for different concentrations of inhibitor was evaluated from potentiodynamic polarization measurements. The data was applied to various isotherms including Langmuir, Temkin, Frumkin and Flory–Huggins isotherms. It was found that the data fit best with the Langmuir adsorption isotherm according to which, the surface coverage (θ) is related to the inhibitor concentration C_{inh} by the equation (10) [28]:

$$\frac{C_{inh}}{\theta} = \frac{1}{K} + C_{inh}$$

(10)

Where K is the adsorption/desorption equilibrium constant, C_{inh} is the corrosion inhibitor concentration in the solution, and (θ) is the surface coverage, which is calculated using equation(11) [29]:

$$\theta = \frac{\eta(\%)}{100}$$

(11)

Where $\eta(\%)$ is the percentage inhibition efficiency as calculated using equation (1). The plot of C_{inh}/θ Vs C_{inh} gave a straight line with an intercept of 1/K. The Langmuir adsorption isotherms [38] for the adsorption of inhibitor on the 6063 aluminium alloy surface are shown in Fig. 8.
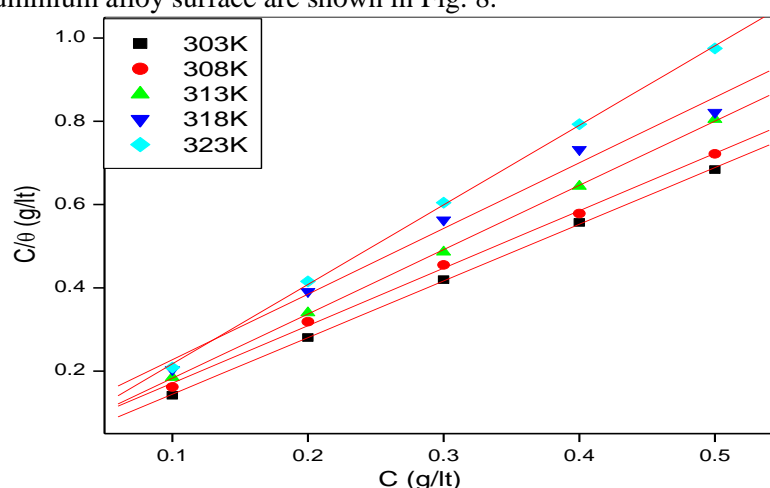

Figure 8: Langmuir adsorption isotherms for the adsorption of *Coriandrum sativum* L. on 6063 aluminium alloy in 1M phosphoric acid at different temperatures

The slopes of the isotherms show deviation from the value of unity as would be expected for the ideal Langmuir adsorption isotherm equation. This deviation from unity may be due to the interaction among the adsorbed species on the metal surface. The Langmuir isotherm equation is based on the assumption that adsorbed molecules do not interact with one another, but this is not true in the case of organic molecules having polar atoms or groups which are adsorbed on the cathodic and anodic sites of the metal surface. Such adsorbed species may interact by mutual repulsion or attraction. It is safely recommended to not determine ΔG_{ads} values since the mechanism of adsorption remains unknown [39].

3.6 Scanning electron microscope studies (SEM) and Energy-dispersive X-ray spectroscopy (EDS) analysis
The SEM images of freshly polished surface of 6063 aluminium alloy is given in Fig. 9 It shows un-corroded surface with few scratches due to polishing. The surface morphology of the 6063 aluminium alloy sample was examined by SEM immediately after corrosion tests in 1.0M phosphoric acid medium. The SEM image of corroded sample in Fig. 10 shows degradation of alloy. Close observation of SEM images indicates the deposition of precipitates on the surface of 6063 aluminium alloy. It may be attributed to deposition of the phase

Deepa and Padmalatha

Mg_5Al_8 which makes an anodic phase in the aluminium matrix resulting in uniform attack and making it an optimum region of dissolution [40]. Fig. 11 represents the inhibitor film on the surface of metal due to the CSE inhibitor.
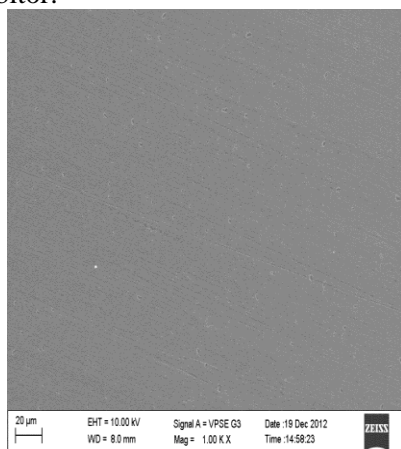
Figure 9: SEM image of freshly polished surface of the 6063 aluminium alloy
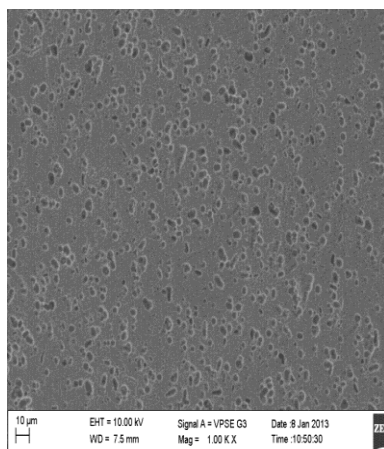
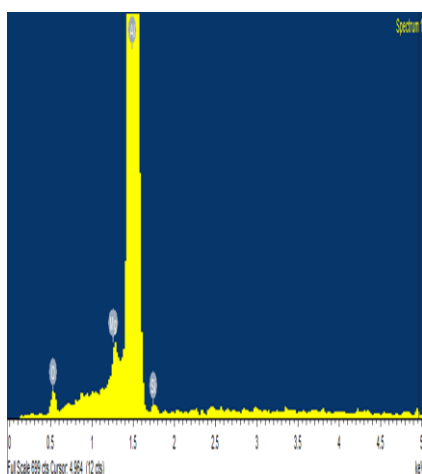**Figure 10:** SEM image of 6063 aluminium alloy after immersion in 1.0M H_3PO_4
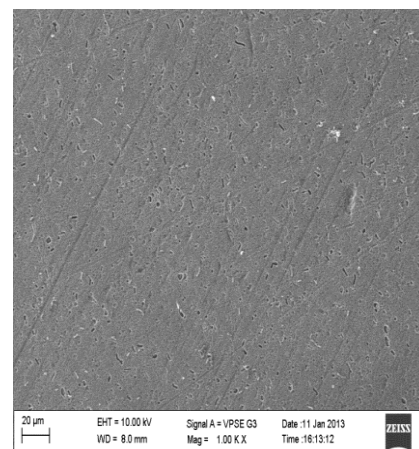
Figure 11: SEM image of 6063 aluminium alloy after immersion in presence of CSE

Table 5 gives the EDS analysis result of 6063 aluminium alloy, 6063 aluminium alloy in 1.0 M Phosphoric acid in the absence and presence of CS inhibitors. Figure 12 represents EDX spectrum of the un-corroded sample of presence of aluminium oxide/hydroxide. Figure 13 depicts the EDX spectrum for the 6063 aluminium alloy. The spectrum shows peaks for aluminium and oxygen suggesting the corroded sample in presence of phosphoric acid. The spectrum shows peaks for aluminium and oxygen suggesting the presence of aluminium oxide/hydroxide. Figure 14 depicts the EDX spectrum for the inhibited sample in presence of CSE.

Table 5: EDS analysis result of 6063 Al in 1M H_3PO_4 in the absence and presence of CS inhibitors
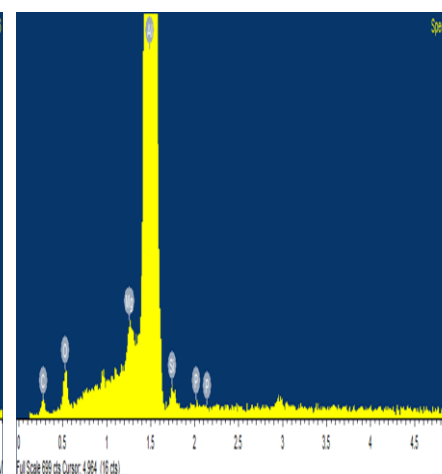
Medium	Composition (%)					
	Al	O	Si	Mg	P	C
6063 aluminium alloy	94.70	4.60	0.45	0.25	-	-
6063 aluminium alloy in 1.0M phosphoric acid	94.73	4.34	0.54	0.30	0.09	-
6063 aluminium alloy in 1.0M phosphoric acid in CS	78.94	6.32	0.55	0.29	0.04	13.86

Figure 12: EDX spectrum of the un-corroded sample of the 6063 aluminium alloy
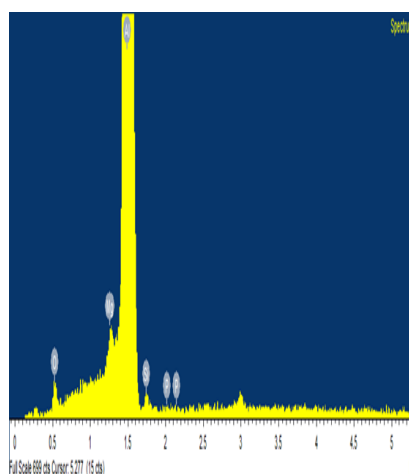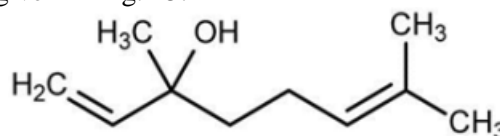

Figure 13: EDX spectrum of 6063 aluminium alloy after immersion in 1.0M H_3PO_4

Figure 14: EDX spectrum of 6063 aluminium alloy after immersion in presence of CSE

741

3.7 Explanation for inhibition
CSE is composed of numerous naturally organic heterocyclic compounds. Major constituent are reported [41] to be Linalool the structure of same is given in Fig. 15.

Figure 15: Structure of Linalool

Surface of 6063 aluminium alloy is covered with thin layer of γ alumina which initially thickens on exposure to neutral aqueous solution with the formation of a layer of crystalline hydrated alumina [42]. The aluminium surface has positive charge in acidic environment in contact with phosphoric acid medium [41]. CSE acts as a mixed type of inhibitor, by bringing both anodic and cathodic reaction under control. At anodic region, hetero atom oxygen present in the molecule may form chelating complex. According to the literature molecules with hydroxyl groups, can readily form complexes with divalent and trivalent ions [43-44]. There will be interaction between the high electron rich oxygen atom of the hydroxyl group and tri-positively charged aluminium [44]. The complex formed will form a barrier between metal and the corrosive environment. In the cathodic region the inhibitor molecule will get adsorbed by weak force of attraction in the form of film formation. The inhibition act of CSE is mainly attributed to the presence of Oxygen heteroatom in the molecule. Thus inhibitor gets adsorbed on the surface of aluminium and a protective film is formed, which reduces the overall corrosion rate. Enhanced corrosion inhibition is also due to the π electrons of the aromatic ring of other constituents of the extract which also act as a rich source of electron.

Conclusion
The main conclusions drawn from this study are:
- CSE is a good eco-friendly green inhibitor for the corrosion control of 6063 aluminum alloy in 1M phosphoric acid solution.
- Inhibition efficiency of the CSE increases with increase in the concentration of the inhibitor.
- Inhibition efficiency of the CSE decreases with increase in the temperature.
- No significant shift in the corrosion potential with addition of inhibitor indicates that CSE acts as mixed inhibitor.
- The adsorption of CSE on the surface of aluminum follows Langmuir adsorption isotherm and undergoes physical adsorption.
- CSE is not only non-toxic and environmental friendly inhibitor, but also inexpensive and renewable source.

Acknowledgements

References
1. Vargel C., Corrosion of Aluminum, Oxford, Elsevier, 2004.
2. Davo, B., de Damborenea, J.J., *Electrochem Acta.* 49(2004) 4957.
3. Ghoneim A. A., Ameer M. A., Fekry A. M., *Int. J. Electrochem. Sci.* 7 (2012)10851.
4. Badawy W.A., Al-Kharafi F.M., El-Azab A.S., *Corros. Sci.* 41(1999)709.
5. Grubac Z., Babic R., Metikos-Hukovic M., *J. Appl. Electrochem.* 32(2002)431.
6. Elewady G.Y., El-Said I.A., Fouda A.S., *Int. J. Electrochem. Sci.* 3(2008)177.
7. Amin M A., Mohsen Q., Hazzai O. A., *Mater. Chem. Phys.* 114 (2009) 908.
8. Noor E., *Corros. Sci.* 47(2005)33.
9. Wang L., *Corros. Sci.* 48(2006)608.
10. Sanyal B., *Prog.Org coat.* 9 (1981) 165.
11. Bentiss F., Traisnel M., Lagrenee M., *Corros. Sci.* 42 (2000) 127.
12. Arab S. T., Noor E. A., *Corrosion* 49 (1993) 122.
13. Luo H., Guan Y.C., Han K.N., *Corrosion* 54 (1988) 721.

14. Lagrenee M., Memari B., Chaibi N., Traisnel M., Vezin H., Bentiss F., *Corros. Sci.*43 (2001) 951.
15. Raja P.B., Sethuraman M.G., *Mater Letts*, 62 (2008) 113.
16. Sangeetha M. et al, *Protection of materials*, 52 (2011) 3.
17. Ambrish Singh, Singh V. K., Quraishi M. A., *J. Mater. Environ. Sci.* 1 (3) (2010) 162.
18. Md. Nazrul Islam Bhuiyan1, Jaripa Begum, Mahbuba Sultana, *Bangladesh J Pharmacol*, 4 (2009)150.
19. Barakat Y. F., Hassan A. M., Herr, Baraka A. M., *Mat. Sci. Eng. Techn.*, 29(7) (1998) 365.
20. Sukhdev Swami Handa, Sumanpreet Singh Khanuja, Gennaro Longo, Devdutt Rakesh, Extraction Technologies for Medicinal and Aromatic Plants, International Centre for Science and High Technology, Trieste, 2008.
21. Sangeetha M., Rajendran S., Sathiyabama J., Krishnaveni A., Shanthy P., Manimaran N., Shyamaladevi B., *Portugaliae Electrochimica Acta* , 29 (6) (2011) 429.
22. Ashok Kumar, Iniyavan P., Saravana Kumar M., Sreekanth A., *J. Mater. Environ. Sci.* 3 (2012) 461.
23. Poornima T., Nayak J., Shetty A.N., *J. Appl. Electrochem*, 41 (2011) 223.
24. Geetha Mable Pinto, Jagannath Nayak, Nityananda Shetty A., *Mat. Chem. Phys.*, 125 (2011) 628.
25. Lagrene N., Mernari B., Bouanis M., Traisnel M., Bentiss F., *Corros. Sci.*, 44 (2002) 573.
26. Brett, C.M.A., *J. Appl. Electrochem.*, 20(6) (1990) 1000.
27. Umoren S.A., Obot I.B., Ebenso E.E., Okafor P.C., *Anti-Corros. Meth &Mater*, 53(2006) 277.
28. Obot I.B., Umoren S. A, Obi-Egbedi N.O., *J. Mater. Environ. Sci.* 2 (1) (2011) 60.
29. Sanat kumar B.S, Nayak J., Shetty A. N., *Journal of Coatings Technology and Research*, 4 (2011) 1.
30. Abdel-Gaber A. M., Abd-El-Nabey B. A., Sidahmed I. M., El-Zayady A. M., Saadawy M., *Corros. Sci.*, 48 (2006) 2765.
31. Sanaa T.A., *Mater. Res. Bull.*, 43(2008) 510.
32. Shivakumar S.S., Mohana K.N., *J. Mater. Environ. Sci.* 4 (3) (2013) 448.
33. Putilova I.N., Balezin S.A., Barannik V.P., Metallic Corrosion Inhibitors, Pergamon Press, New York, 1960, 31.
34. Bentiss F., Lebrini M., Lagrenee M., *Corros. Sci.*, 47 (2005) 2915.
35. Oguzie E.E., *Corros. Sci.*, 49 (2007) 1527.
36. Martinez S., Stern I., *Appl. Surf. Sci.*, 199 (2002) 83.
37. Marsh J., Advanced Organic Chemistry, third ed., Wiley Eastern, New Delhi, 1988.
38. Hammouti B., Zarrouk A., AL-Deyab S.S., Warad I., *Oriental Journal of Chemistry*, 27 (1) (2011) 23.
39. Benali O., Benmehdi H., Hasnaoui O., Selles C., Salghi R., *J. Mater. Environ. Sci.* 4 (1) (2013) 127.
40. Awady A. A., Abd, El- Nabey B.A., Aziz S.G., *J. Chem. Soc. Faraday Trans.*, 89 (1993) 795.
41. Md. Nazrul Islam Bhuiyan, Jaripa Begum, Mahbuba Sultana, *Bangladesh J Pharmacol,* 4 (2009) 150.
42. Suma A Rao, Padmalatha, Nayak J., Shetty A.N., *Trasnsactions of SAEST*, 41(2006) 1.
43. Brouillard R., Dangles O., The Flavonids, Advances in research since 1986, Champman & Hall, London, 1993.
44. Abiola O. K., Aliyu A.O.C., Phillips A.A., Ogunsipe A.O., *J. Mater. Environ. Sci.* 4 (2013) 370.

(2013); http://www.jmaterenvironsci.com